Density Functional Investigation on α-MoO 3 (100): Amines Adsorption and Surface Chemistry

Tingqiang Yang, Shuang Yang, Wei Jin, Yule Zhang, Nicolae Barsan, Anne Hémeryck, Swelm Wageh, Ahmed Al-Ghamdi, Yueli Liu, Jing Zhou, et al.

Density Functional Investigation on Alpha-MoO_3 (100): Amines Adsorption and Surface Chemistry

Tingqiang Yang,[a,b,d,] Shuang Yang,[b] Wei Jin,[c] Yule Zhang,[d] Nicolae Barsan,[e] Anne Hemeryck,[f] Wageh Swelm,[g] Ahmed A. Al-Ghamdi,[g] Yueli Liu,[c] Jing Zhou,[b] Wen Chen,[b,]* and Han Zhang[d,]**

[a]Postdoctoral Innovation Practice Base of Guangdong Province, Hanshan Normal University, Chaozhou, 521041, China

[b]State Key Laboratory of Advanced Technology for Materials Synthesis and Processing, School of Materials Science and Engineering, Wuhan University of Technology, Wuhan, 430070, China

[c]State Key Laboratory of Silicate Materials for Architectures, School of Materials Science and Engineering, Wuhan University of Technology, Wuhan, 430070, China

[d]Institute of Microscale Optoelectronics, Collaborative Innovation Centre for Optoelectronic Science & Technology, Key Laboratory of Optoelectronic Devices and Systems of Ministry of Education and Guangdong Province, College of Physics and Optoelectronic Engineering, Shenzhen Key Laboratory of Micro-Nano Photonic Information Technology, Guangdong Laboratory of Artificial Intelligence and Digital Economy (SZ), Shenzhen University, Shenzhen, 518060, China

[e]Institute of Physical and Theoretical Chemistry and Center for Light-Matter Interaction, Sensors & Analytics (LISA+), University of Tübingen, D-72076 Tübingen, Germany

[f]LAAS-CNRS, Université de Toulouse, CNRS, F-31555 Toulouse, France

[g]Department of Physics, Faculty of Science, King Abdulaziz University, Jeddah 21589, Saudi Arabia

*Corresponding author:

Dr. Tingqiang Yang: yang_tq@szu.edu.cn

Prof. Wen Chen: chenw@whut.edu.cn

Prof. Han Zhang: hzhang@szu.edu.cn

Abstract

The (100) surface of alpha-MoO_3 (α-MoO_3) should possess overwhelmingly more exposed Mo than the (010), and the exposed Mo has been extensively considered as active site for amine adsorption. However, α-MoO_3 (100) has drawn little attention concerning amine sensing mechanism. In this research, adsorption of ammonia (NH_3), monomethylamine (MMA), dimethylamine (DMA), and trimethylamine (TMA) is systematically investigated by density functional theory (DFT). All of these four molecules have high affinity to α-MoO_3 (100) through interaction between the N and the exposed Mo, and the affinity is mainly influenced by number of methyl group and number of N-connected H. Adsorption and dissociation of water and oxygen molecule on stoichiometric or defective α-MoO_3 (100) surface are then simulated to fully understand surface chemistry of α-MoO_3 (100) in practical condition. At low temperature α-MoO_3 (100) must be covered with lots of water molecule; the water can desorb or dissociate into hydroxyl groups at high temperature. Oxygen vacancy (V_O) can be generated considering the annealing process during sensor device fabrication; V_O must be filled with O_2 molecule, which can further interact with adsorbed water nearby to form hydroxyl groups. According to this research, α-MoO_3 (100) must be the active surface for amine sensing and its surface chemistry is well understood. In near future, further reaction and interaction will be simulated at α-MoO_3 (100), and much more attention should be paid to α-MoO_3 (100) not only theoretically but also experimentally.

Key words

DFT; α-MoO_3 (100); amines adsorption; surface chemistry; gas sensing

TOC Graph

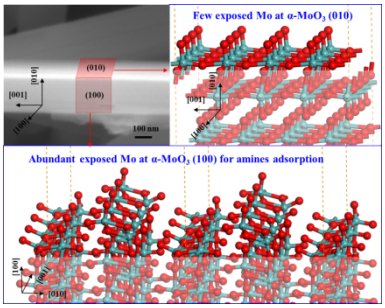
Few exposed Mo at α-MoO3 (010)
(010)
(100)
100 nm
Abundant exposed Mo at α-MoO3 (100) for amines adsorption

1. Introduction

Alpha-MoO_3 (α-MoO_3) has drawn intensive attention in gas sensor mainly because of its outstanding sensing performance for amine gases, such as ammonia (NH_3), trimethylamine (TMA) and triethylamine.[1-7] In our previous research, α-MoO_3 nanobelts have been prepared and have shown extremely high response and superb selectivity to TMA.[1] For sensing reactions at α-MoO_3 surface, the TMA was considered to be oxidized by lattice oxygen of α-MoO_3 into N_2, CO_2 and H_2O according to gas chromatography.[1] In term of active site for amines adsorption at α-MoO_3 surface, it has been extensively believed that the N atom of amines interacts with exposed Mo atom at surface through coordination between the lone-pair electrons of N and empty 4d orbital of Mo.[2-5]

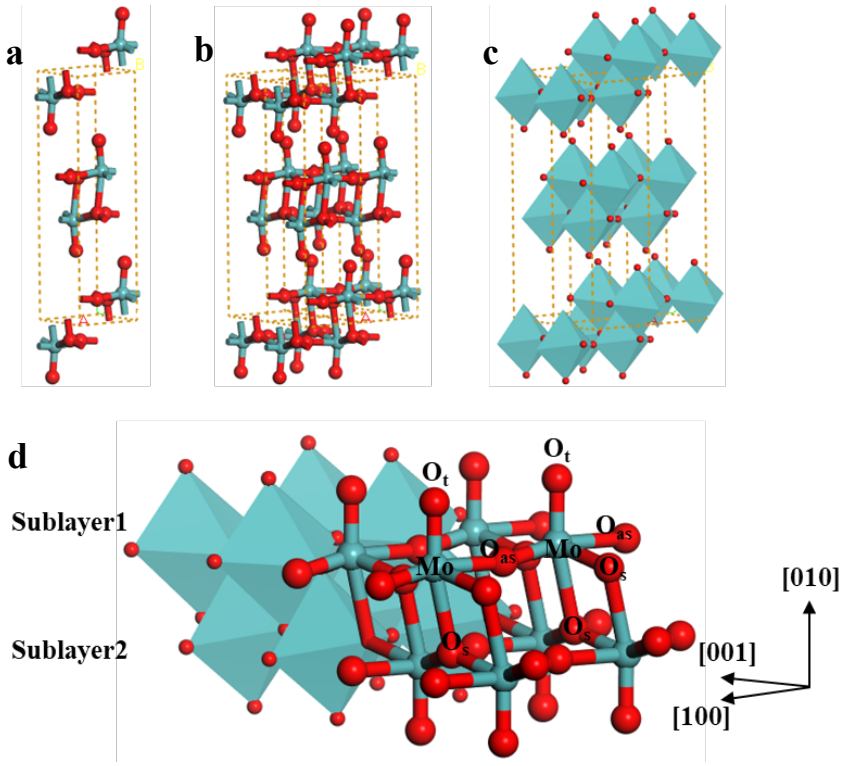

Figure 1 (a) Primitive cell of α-MoO_3; primitive cell in (b) ball-stick and (c) polyhedron display style showing four periodic lattices in [100] and [001] directions; (d) bilayer MoO_6 octahedrons demonstrating three structurally distinct oxygen atoms (O_t, O_{as}, and O_s).

Crystalline MoO_3 has three polymorphs with orthorhombic phase (α-MoO_3) being thermodynamically stable. As shown in Figure 1, orthorhombic α-MoO_3 crystal is comprised of stacked bilayers of distorted

MoO_6 octahedrons through weak van der Waals interaction along the [010] direction, and the octahedrons inside the bilayer connect by sharing vertices along the [100] direction and by sharing edges along the [001] direction.[8] There are three structurally distinct oxygen atoms in each octahedron, i.e. single-coordinated terminal oxygen (O_t) forming the shortest bond with Mo, the double-coordinated asymmetric oxygen (O_{as}) respectively forming one long and one short bond with two Mo, and the triple-coordinated symmetric oxygen (O_s) forming two equal short bonds with two Mo in the same sublayer and one longest bond with Mo in the other sublayer, as shown in Figure 1d.

The weak interaction between the layers usually results α-MoO_3 nanomaterials in sheet- or belt-like morphology with the (010) plane being the most exposed surface. Similarly, our previous α-MoO_3 nanobelts are dominantly exposed with the (010) plane. At the same time, it is worth noting that (100) plane also takes up a large portion for the nanobelt, and (001) can be ignored.[1]

Because of highest percentage of (010) plane at α-MoO_3 surface, α-MoO_3 (010) has been experimentally and theoretically investigated for a long period. **Figure S1a** shows the atomic structure of the α-MoO_3 (010) surface. It is reasonable that the geometry of the surface (010) is identical to that inside the bulk because all of O_t at (010) plane are singly coordinated with Mo and no bond needs to be broken to form α-MoO_3 (010) surface.[9] Although Kwak et al. have theoretically demonstrated that NH_3 adsorption on the oxygen vacancy site of α-MoO_3 (010) surface is much more feasible than stoichiometric one,[2] both experimental and theoretical result have demonstrated that the oxygen vacancy, especially O_t vacancy (V_{Ot}), is unstable or difficult to be generated.[2, 10-11] In early 1983, Firment et al. have studied stoichiometric and oxygen deficient α-MoO_3 (010) surface, demonstrating that the oxygen deficient surface is unstable.[10] In 2007, Cavalleri et al. have revealed the characteristic of V_O at α-MoO_3 (010) by combining angle-resolved near-edge X-ray absorption fine structure (NEXAFS) with density functional theory (DFT), and demonstrated that the relaxation of V_{Ot} can make O_{as} replace the original O_t.[11] Some theoretical calculation has verified the result by Cavalleri et al., demonstrating that the O_{as} beside the O_t takes the place of the original O_t if there is one V_{Ot}.[12-14] Even though other theoretical research has reported that O_{as} can stay at its original place when O_t is removed,[15-16] there is little dispute that the formation energy of V_{Ot} is so high that it is difficult to generate abundant O_t vacancies at α-MoO_3 (010). Therefore, it is not advisable to consider α-MoO_3 (010) as active surface for amines adsorption.

As mentioned, α-MoO_3 (100) plane also takes up a large portion of the surface, especially for our nanobelts.[1] **Figure S1b** shows the atomic structure of α-MoO_3 (100) surface, which is identically cleaved according to other theoretical research. [9, 13] It is clear that half of the α-MoO_3 (100) surface is exposed with Mo atoms. According to field emission scanning electron microscope (FESEM) images of our α-MoO_3 nanobelts, the width/thickness ratio of the nanobelts is even smaller than 10, as shown in **Figure S2**. Additionally, the formation energy of V_{Oas} at α-MoO_3 (100) is lower than that of V_{Ot} at α-MoO_3 (010), which means V_{Oas} is even easier to be generated at α-MoO_3 (100).[13] Therefore, the α-MoO_3 (100) must possess overwhelmingly more exposed Mo atom at than the (010) for our nanobelts.

Actually, α-MoO_3 (100) has already drawn some interest in olefin catalysis field.[17-18] Papakondylis et al. have theoretically explored the adsorption of H_2O and CO on α-MoO_3 (100).[9] However, little attention has been paid to amine adsorption at α-MoO_3 (100). the theoretical research by Papakondylis et al. in early 1996 is still far from understanding the surface chemistry of α-MoO_3 (100) under gas sensing measurement condition.

In this work, for the first time, amines adsorption at α-MoO_3 (100) surface is theoretically investigated by density functional calculation. The adsorption energy and charge transfer of NH_3, monomethylamine (MMA), dimethylamine (DMA), and TMA are calculated and compared. Additionally, to fully understand surface chemistry of α-MoO_3 (100) under amine sensing measurement condition, the adsorption and dissociation of water and oxygen molecule on stoichiometric or defective α-MoO_3 (100) surface are simulated.

2. Computational details

Spin-unrestricted DFT calculations within a periodic supercell were performed by Dmol3 package.[19-20] General gradient approximation (GGA) in the form of a Perdew–Burke–Ernzerhof (PBE) was selected for the exchange–correlation functional, and a DFT-D correction was executed to consider van der Waals interaction among bilayers of α-MoO_3 as well as the weak interaction between gas molecules and α-MoO_3 surface. The inner electrons of Mo were replaced by an effective core potential (ECP), and electrons of others are in all-electron calculation. The Hubbard parameter, U, was set as 2 eV to treat the coulomb interaction among d-orbital electrons of Mo. A 9 × 3× 9 or 3 × 3 × 1 Monkhorst–Pack grid was respectively used for Brillouin-zone integrations of α-MoO_3 primitive cell and α-MoO_3 (100) supercell. For geometry

optimization, convergence tolerance is 2×10^{-5} hartree in energy, 4×10^{-3} hartree $Å^{-1}$ in force, and 5×10^{-3} Å in displacement. For transition state (TS) search, a linear synchronous transit/quadratic synchronous transit (LST/QST) method was used with root-mean-square (RMS) convergence of 0.01 hartree/Å.

The adsorption energy (E_{ads}), formation energy of V_O ($E[V_O]$), activation energy (E_a) and reaction energy (E_{react}) are defined as

$$E_{ads} = [E_{\alpha\text{-}MoO3\ (100)+\ n\ gas} - E_{\alpha\text{-}MoO3\ (100)} - n\ E_{gas}]/n \quad \textbf{Equation 1a}$$

$$E[V_O] = E_{\alpha\text{-}MoO3\ (100)\_VO} + 1/2\ E_{O2} - E_{\alpha\text{-}MoO3\ (100)} \quad \textbf{Equation 1b}$$

$$E_a = E_{TS} - E_{reactant} \quad \textbf{Equation 1c}$$

$$E_{react} = E_{procuct} - E_{reactant} \quad \textbf{Equation 1d}$$

Herein, in **Equation 1a** $E_{\alpha\text{-}MoO3\ (100)+\ n\ gas}$, $E_{\alpha\text{-}MoO3\ (100)}$ or E_{gas} represent the total energy of α-MoO_3 (100) with gas molecules adsorbed, the total energy of α-MoO_3 (100) or that of a specific gas molecule, and n is the number of adsorbed molecule. Similarly, in **Equation 1b**, $E_{\alpha\text{-}MoO3\ (100)\_VO}$ and E_{O2} represent the total energy of α-MoO_3 (100) with one oxygen vacancy and that of one oxygen molecule. In **Equation 1c and 1d**, $E_{reactant}$, E_{TS} or $E_{procuct}$ means the energy at the beginning, transition state or end of a reaction. Accordingly, a negative value of E_{ads} or E_{react} corresponds to an exothermic adsorption or reaction. To analyze the charge transfer between the surface and adsorbed molecules, Mulliken charge was calculated. The unit of Mulliken charge is the absolute value of elementary electron charge, thus the positive value of adsorbed molecule means electron donation from the molecule to α-MoO_3 surface.

The optimized orthorhombic α-MoO_3 possesses lattice parameters of a = 3.95 Å, b = 13.86 Å and c = 3.74 Å, which is very close to experimental value of a = 3.96 Å, b = 13.86 Å and c = 3.69 Å.[13, 21] Based on the optimized α-MoO_3 primitive cell, a (1 × 4) supercell of α-MoO_3 (100) surface was cleaved, as shown in **Figure S1b and Figure S2**. The supercell is in size 13.86 × 14.95 × 37.36 $Å^3$ with 240 O atoms and 80 Mo atoms in total. A 15 Å vacuum layer is introduced to avoid interaction among the slabs in [100] direction and some bottom atoms were fixed to simulate bulk atoms, which is red color in **Figure S3**. The α-MoO_3 (100) surface is not smooth but with terrace and channel because of interlaced stacking of octahedron bilayers along [010] direction. To clearly show the terrace-channel peculiarity of the α-MoO_3 (100) surface, the supercell is presented with two periodic lattices along [010] direction.

3. Results and discussion

Amines adsorption at stoichiometric α-MoO_3 (100) surface

With assurance of α-MoO_3 (100) being active surface for amines adsorption, DFT calculation was performed to investigate adsorption site, adsorption energy and charge transfer for four amines, i.e. NH_3, MMA, DMA, and TMA. **Figure 2a and b** shows adsorption configurations of NH_3 at terrace of α-MoO_3 (100). It is similar to what has been believed that N atom bonds to the exposed Mo atom by offering its lone-pair electron to the empty 4d orbital of Mo. Additionally, two H atoms of NH_3 may have hydrogen bond interaction with adjacent O_{as}. The adsorption energy is −1.47 eV, suggesting high ability of α-MoO_3 (100) to adsorb NH_3. **Figure 2c-h** shows the adsorption configurations of MMA, DMA, and TMA at terrace of α-MoO_3 (100). All of these adsorptions mainly originate from the interaction between the N and exposed Mo. Nevertheless, there are still some differences. As listed in **Table 1**, comparisons are made on the adsorption energy, the N−Mo distance and the charge transfer of these amines. For the adsorption at terrace, E_{ads} (in absolute value) increases with the number of methyl groups increasing from 0 to 2, i.e. from NH_3 to DMA, while E_{ads} decreases when it goes to 3, i.e. TMA. The increase from NH_3 to DMA can be mainly ascribed to electron-releasing effect of methyl group. The N atom is more electron-abundant in the amine molecule with more methyl group, which renders N atom more affinitive to Lewis site of Mo. Additionally, heavier molecule somehow facilitates van der Waals interaction. In term of the E_{ads} reduction from DMA to TMA, it can be ascribed to the three methyl groups which have a repulsive effect with the surface bonds and prevent the N to coordinate with Mo. Hence, the distance between the N and Mo is 2.558 Å, longer than that of the others, as shown in **Table 1**. Furthermore, the low E_{ads} also results from the lack of hydrogen bond interaction between TMA, which is has no H atom connected to N, and the surface O_{as}.

The repulsion effect between methyl group and Mo-O_t bond can be verified by comparing two MMA adsorption configurations. **Figure S4** shows MMA adsorption at terrace of α-MoO_3 (100) without or with N−C bond overlapping with Mo−O_t bond. The angle between N−C bond and N−Mo bond (∠CNMo) and the angle between N−Mo bond and Mo−O_t bond (∠$NMoO_t$) is respectively 118.35° and 82.60° in the configuration of **Figure S4a and S4b**. Comparatively, ∠CNMo and ∠$NMoO_t$ is respectively 118.79° and 86.54° in the configuration of **Figure S4c and S4d**. The larger angles, especially for the ∠$NMoO_t$, demonstrate a more severe repulsion in the latter configuration. The adsorption energy for the former (−1.70 eV) is slightly higher than its counterpart (−1.68 eV) despite that one less hydrogen bond can be

formed. Accordingly, the repulsion effect between methyl group and Mo−O_t plays a more important role than the hydrogen bond interaction for the MMA adsorption. It is also for this reason that the N−C bond does not overlap with the Mo−O_t bond for the adsorption of DMA and TMA, as shown in **Figure 2e-h**.

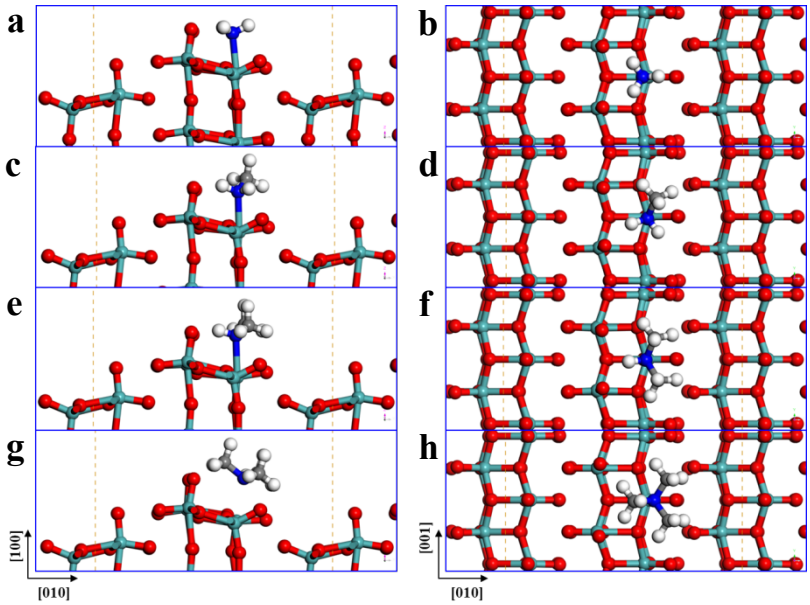

Figure 2 Adsorption configuration at terrace of α-MoO_3 (100): (a, b) NH_3, (c, d) MMA, (e, f) DMA, and (g, h) TMA.

Table 1 Adsorption energy, distance between the N and the Mo, and Mulliken charge for amines adsorbed at terrace or channel site of α-MoO_3 (100).

Amines		NH_3	MMA	DMA	TMA
Number of methyl group		0	1	2	3
E_{ads} (eV)	Terrace	−1.47	−1.70	−1.77	−1.37
	Channel	−1.66	−1.80	−1.69	−1.36
N-Mo (Å)	Terrace	2.343	2.345	2.401	2.558
	Channel	2.338	2.346	2.442	3.934
Mulliken charge (|e|)	Terrace	0.283	0.308	0.319	0.271
	Channel	0.285	0.301	0.316	0.498

Besides terrace, amine molecules can also be adsorbed at channel, as shown in **Figure S5**. The adsorption energy is also listed in **Table 1**. By comparing the E_{ads} at terrace and channel site, it can be concluded that small amine molecules, such as NH_3 and MMA, tend to be adsorbed at the channel, while

the large molecules, such as DMA and TMA, at terrace. Interestingly, E_{ads} of TMA at channel is very approaching to that at terrace, even though the N is still distant from the Mo (3.934 Å). The reason can be that more H atoms in the methyl groups can interact with more O_{as} and $O_{t.}$ at the surface when TMA is at channel.

The Mulliken charge is also analyzed for each configuration, as listed in **Table 1**. Firstly, they are all positive, suggesting electron donation from adsorbed amines to α-MoO_3 (100) surface. Secondly, comparing the Mulliken charge of the four amines at terrace, we find that DMA donates electron at most, followed by MMA, NH_3 and TMA, which shows the same trend as E_{ads}. Nevertheless, for TMA at channel, the Mulliken charge reaches 0.498 |e|, much higher than others. As mentioned before, it can be attributed to the interaction between the H atoms in the methyl group with the surface O_{as} and O_t. Except TMA, the Mulliken charge at channel is slightly higher than that at terrace.

Based on above result, the amine molecules are highly affinitive to α-MoO_3 (100) surface and can donate many electrons once adsorbed. This somehow can explain why the resistance of n-type α-MoO_3 decreases when amine gas is injected.[1-7, 22] However, adsorption is only the first step for gas sensing reaction, and continuous dissociation or reaction at the surface can be more significant for understanding sensing mechanism.

O_2, H_2O, and V_O at α-MoO_3 (100) surface

Instead of continuing to simulate decomposition or reaction of these adsorbed amines, we would like to investigate the surface chemistry of at α-MoO_3 (100) with taking O_2, H_2O and V_O into consideration. It must be kept in mind that there is never a perfect surface. It is necessary to consider whether and how can Mo sites be exposed under gas sensing measurement condition, in which a large number of O_2 and H_2O molecules must interact with the surface. O_2 concentration in air is about 21 % (210,000 ppm) and H_2O concentration at 50 % relative humidity at 25 °C is about 10, 000 ppm,[23] which are both much higher than amine concentration in sensing measurement.

The effect of the oxygen molecule in air cannot be excluded for understanding gas sensing mechanism. For some metal oxides, reducing gas is believed to be oxidized by adsorbed oxygen, but for some others, it is lattice oxygen.[24-29] Lattice oxygen of α-MoO_3 is abundant and active, and some have believed it is lattice oxygen that oxidize reducing gas molecules,[1, 6] while others adsorbed oxygen.[5, 7] Hence, the O_2 adsorption

at stoichiometric α-MoO_3 (100) is simulated, as shown in **Figure S6**. It is found that E_{ads} is 0.57 eV and 0.47 eV for adsorption at terrace and channel site of α-MoO_3 (100) and O_2 molecule is still of ~3 Å distance from the exposed Mo site. Therefore, O_2 adsorption on stoichiometric α-MoO_3 (100) surface is not favorable.

As mentioned before, humidity has also to be considered. It has been discovered that H_2O molecule has huge effects on gas sensing properties of metal oxides, and certainly for α-MoO_3.[1, 30-32] Water adsorption at α-MoO_3 (100) has already been theoretically investigated, and it has found that E_{ads} is about −1 eV for full coverage of H_2O (each exposed Mo with one H_2O molecule).[9] Herein, H_2O adsorption at α-MoO_3 (100) in different coverages (1/8, 1/4, 1/2 and full) as well as its dissociation are simulated, as shown in **Figure 3**. The adsorption energy and Mulliken charge of these configurations are listed in **Table 2**. The result demonstrates that water molecule tends to be adsorbed at channel site at low coverage (1/8 and 1/4) with its O atom bonding to the exposed Mo and its two H atoms having hydrogen bond interaction with surface O_{as}, as shown in **Figure 3a-d**. When the coverage increases to 1/2, the water molecule cannot be entirely adsorbed at channel, and half of them terrace, as shown in **Figure 3e**. **Figure 3f** shows the relaxed configuration of four water molecules at channel site, and it can be found that some of the water molecules rotate a little to a lower-energy state in which one H can interact with O_{as} at channel and the other H can interact with O_t at terrace. This suggests that the hydrogen bond interaction between H atom and the O_{as} at channel is reduced if there are eight H atoms from four water but only four O_{as}. Moving half of water molecules to terrace can render stronger hydrogen bond interaction. **Figure S7** shows other two possible configurations of 1/2 water, which are also less stable that **Figure 3e**. The rotation of water at channel is also found for fully covered α-MoO_3 (100), as shown in **Figure 3g and h**. The configuration in **Figure 3g** with three water rotating is somewhat more stable than that in **Figure 3h** with only one rotating molecule. Notably, when the three rotate, the remaining molecule does not need to rotate because it can have full hydrogen bond interaction with two O_{as} at channel. None of four water molecules at terrace rotate because none of O_t from channel is at same height as the H atoms and to interact with them. As for the Mulliken charge, they are all positive, meaning the water adsorption can also result in resistance reduction for n-type α-MoO_3, which has already been verified by our previous research.[1] From **Table 2**, it can also be seen that less electronic effect is induced as the number of adsorbed water molecules increases.

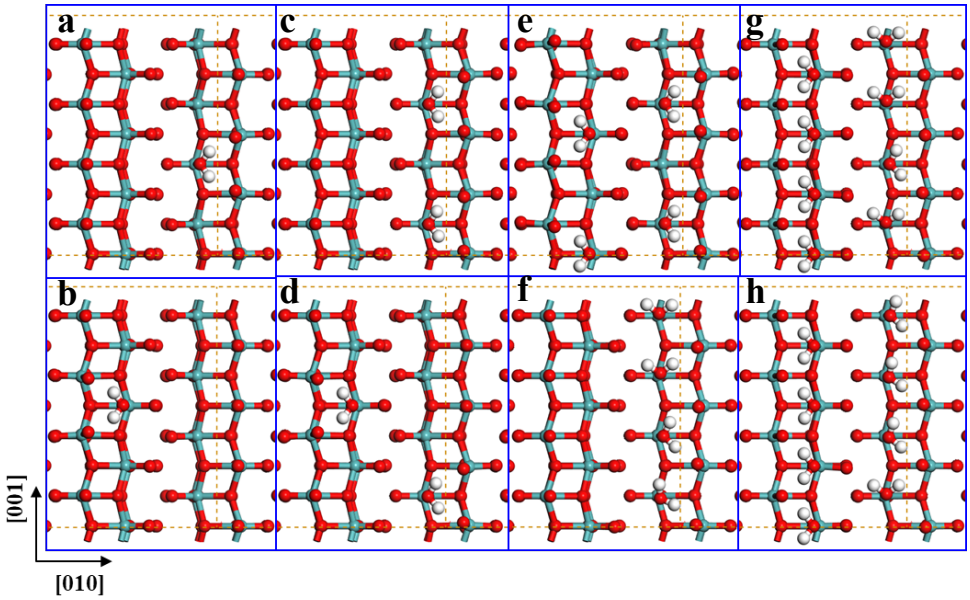

Figure 3 Water adsorption at α-MoO_3 (100) in (a, b) 1/8, (c, d) 1/4, (e, f) 1/2 and (g, h) full coverage: (a) At channel and (b) at terrace site; (c) two both at channel and (d) one at channel and the other terrace; (e) all at channel and (f) two at channel and the others at terrace; (g, h) the water molecules adsorbed at channel in different configuration.

Table 2 Average adsorption energy and Mulliken charge for one water molecule at α-MoO_3 (100) in different coverage (Superscripts of a-h represents the configuration in **Figure 3a-h**.)

Coverage	1/8	1/4	1/2	Full
E_{ads} (eV)	-1.20^{a}	-1.19^{c}	-1.16^{e}	-1.14^{g}
	-1.13^{b}	-1.17^{d}	-1.15^{f}	-1.11^{h}
Mulliken charge (|e|)	0.192^{a}	0.187^{c}	0.184^{e}	0.174^{g}
	0.182^{b}	0.187^{d}	0.169^{f}	0.175^{h}

The adsorbed water may also dissociate when temperature is elevated. Herein, dissociation of one water molecule at terrace or channel of α-MoO_3 (100) is simulated. As clearly shown in **Figure 4**, the molecularly adsorbed water is more stable than dissociated water either at terrace or at channel according to the relative energy and energy barrier. Nonetheless, the water molecule at channel takes more possibility to

dissociate with E_a and E_{react} of 0.78 eV and 0.57 eV, compared with 1.05 eV and 0.76 eV at terrace. From the atomic structures on the right, it can be seen that the reason why the dissociated water is more stable at the channel than at the terrace is that the formed HO_{as} group of the former can have hydrogen bond interaction with nearby O_t in terrace with a distance of 2.044 Å.

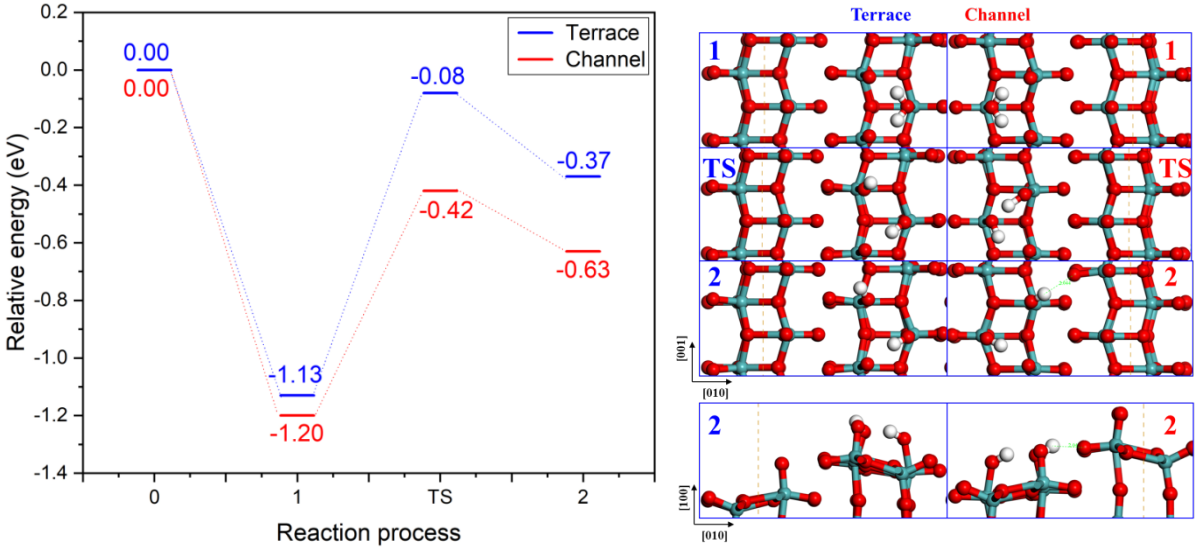

Figure 4 Water dissociation process at terrace and channel of α-MoO_3 (100). The left shows relative energy at each process with reference to overall energy of stoichiometric surface plus vapor water molecule, and the right shows atomic structure in different process.

Based on the calculation of water adsorption, it can be deduced that there must be numerous water molecules previously adsorbed at α-MoO_3 (100) in measurement condition, especially at room or relatively low temperature. The adsorption site for water is same as that for amines, thus the existence of water should prevent the adsorption of amines. However, if working temperature is elevated, some of water molecules may be desorbed, which can provide site for amine adsorption. The water at the terrace is more likely to desorb because the E_{ads} at terrace is somewhat lower than that at channel. In contrast, the molecules at channel the may either be desorbed or dissociate.

Besides O_2 and H_2O, V_O must also be taken into consideration, because the annealing process during material synthesis and device fabrication probably leads to V_O formation.[1] **Figure 5a** shows five kinds of oxygen at α-MoO_3 (100) surface. O_{as}(t) and O_{as}(c) represent O_{as} at terrace and channel, and O_s(t) represents

O_s at terrace. Notably, there are two kinds of O_t even only at the terrace, one of them is connected with fully coordinated Mo, which is labeled O_t(tf), and the other is connected with exposed Mo, which is labeled O_t(te). **Figure 5b-f** shows the relaxed configuration of α-MoO_3 (100) with five different vacancies, i.e. $V_{Oas(t)}$, $V_{Oas(c)}$, $V_{Ot(tf)}$, $V_{Ot(te)}$, and $V_{Os(t)}$, whose vacancy formation energy is respectively 1.23 eV, 1.30 eV, 1.23 eV, 1.35 eV, and 3.75 eV. Interestingly, E[$V_{Oas(t)}$] is same as the E[$V_{Ot(tf)}$], and the underlying reason is that α-MoO_3 (100) with one $V_{Ot(tf)}$ is relaxed to the same configuration as that with one $V_{Oas(t)}$, as can be seen in **Figure 5b and d**. **Movie S1** shows the process more clearly. This process is similar to what has happened at α-MoO_3 (010) in other theoretical research.[11-14] Therefore, $V_{Oas(t)}$ is most likely to generate. The relaxed configuration with $V_{Ot(te)}$ is also very interesting, and **Figure 5e** and **Movie S2** show that the exposed Mo is dragged inside by two O_{as} underneath.

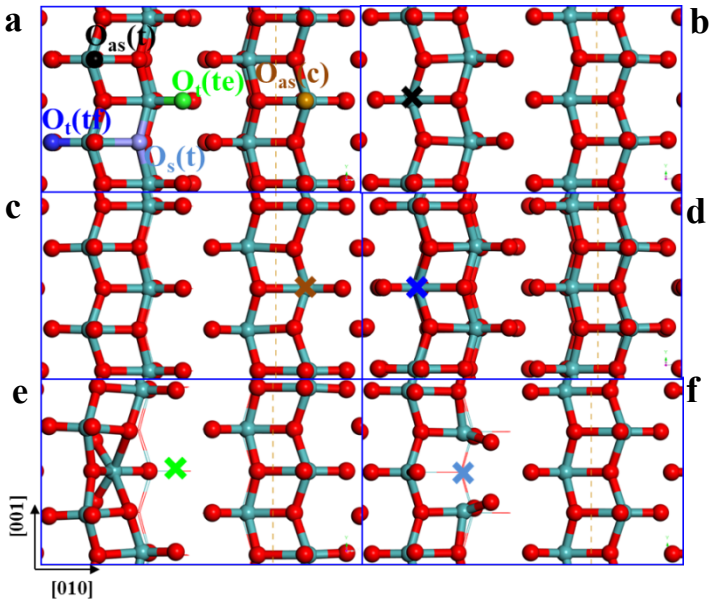

Figure 5 (a) α-MoO_3 (100) surface showing five kinds of oxygen, and (b-f) the relaxed configuration of α-MoO_3 (100) with five different vacancies.

The $V_{Oas(t)}$ may form during annealing process, whereas it has a high tendency to interact with O_2 and H_2O in air after the annealing. **Figure S8** shows adsorption and dissociation process of O_2 at α-MoO_3 (100) with one $V_{Oas(t)}$. Compared with stoichiometric surface, O_2 can be easily adsorbed at $V_{Oas(t)}$ with E_{ads} of −0.63 eV. Once O_2 is adsorbed, the O−O bond elongates from 1.233 Å to 1.363 Å, and Mulliken charge of

O_2 becomes −0.443 |e|, which suggests electron extraction from surface. This implies the tendency of O_2 to dissociate. However, E_a and E_{react} for its dissociation are as high as 1.64 eV and 1.18 eV. It suggests O_2 is hard to dissociate, herein, especially at low temperature. A water molecule may also be adsorbed at or around $V_{Oas(t)}$ site, while the calculation result shows that $V_{Oas(t)}$ does not facilitate adsorption of water. As shown in **Figure S9**, the most favorable adsorption configuration is **Figure S9e and f**, with E_{ads} of −1.06 eV, which is still a little lower than that at stoichiometric surface.

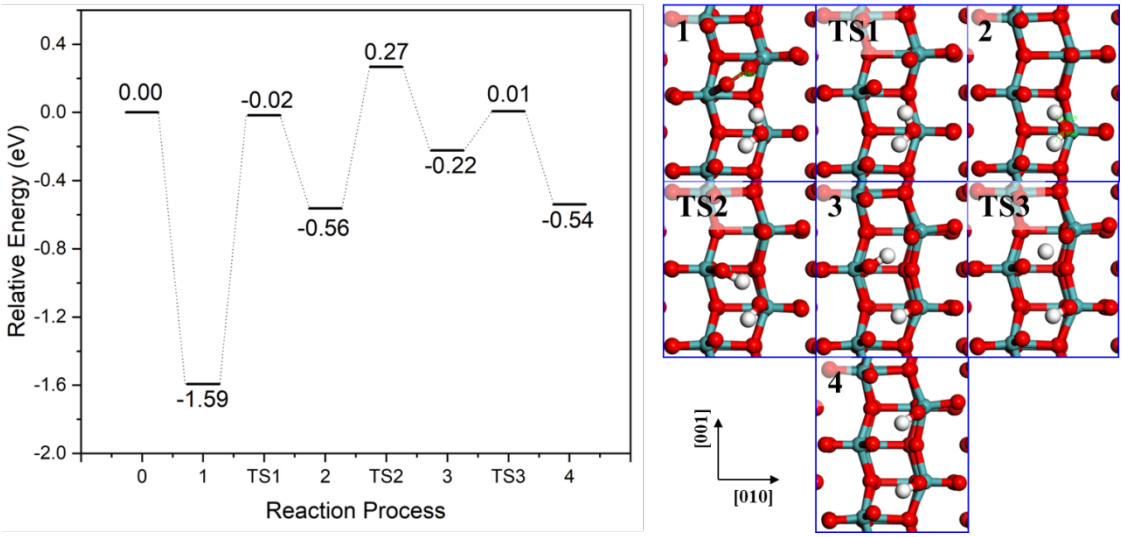

Figure 6 Adsorption and dissociation of both O_2 and H_2O at α-MoO_3 (100) with one $V_{Oas(t)}$. The left shows relative energy at each process with reference to overall energy of defective surface plus vapor O_2 and H_2O molecule, and the right shows atomic structure in different process.

Co-adsorption of O_2 and H_2O around $V_{Oas(t)}$ is also of high possibility, because there are three exposed Mo atoms very close to each other. **Figure 6** shows co-adsorption and dissociation of both O_2 and H_2O at α-MoO_3 (100) with one $V_{Oas(t)}$. The energy for the co-adsorption is −1.59 eV, suggesting the high feasibility, even though it is a little lower than the sum of E_{ads} of single O_2 (−0.63 eV) and single H_2O (−1.06 eV) adsorption at or around $V_{Oas(t)}$. Additionally, the presence of H_2O facilitates the dissociation of O_2 with E_a and E_{react} of 1.57 eV and 1.03 eV, which is respectively 0.07 eV and 0.15 eV lower than those with absence of H_2O. The dissociation of O_2 in turn facilitates dissociation of H_2O. The H−O bond closest to dissociated O_2 elongates to 0.995 Å, and the other 0.990 Å. The former is easier to rupture by transferring the H to the

O_{as}, which is dissociated from O_2, with E_a and E_{react} of 0.83 eV and 0.34 eV. The E_a and E_{react} are 0.22 eV and 0.42 eV lower than those of water dissociation at terrace of stoichiometric α-MoO_3 (100). The HO_{as} is not stable, and the H can be easily (E_a = 0.23 eV) captured by the other O atom dissociated from O_2, reaching a more stable configuration. Finally, α-MoO_3 (100) surface with two terminal hydroxyl groups is formed.

Therefore, in practive, α-MoO_3 (100) must already be covered with lots of water molecule, especially at low temperature. If the temperature is high enough, adsorbed water may dissociate to form a terminal HO and rooted HO_{as} group. Because of the annealing process, $V_{Oas(t)}$ is likely to be generated, but can be easily filled with O_2 molecule. The adsorbed O_2 molecule at $V_{Oas(t)}$ may dissociate with the nearby H_2O, and this finally leads to two terminal hydroxyl groups at surface.

4. Conclusion

It has been rationally analyzed that α-MoO_3 (100) should possess overwhelmingly more exposed Mo than α-MoO_3 (010) based on previous experimental and theoretical investigation. Accordingly, in this research, amines adsorption as well as interaction between O_2, H_2O and V_O at α-MoO_3 (100) surface are systematically investigated by density functional theory calculation. All four amine molecules have high affinity to the α-MoO_3 (100) surface through interaction between the N and the exposed Mo, while the affinity is mainly influenced by number of methyl group, number of N-connected H. Regarding the surface chemistry, α-MoO_3 (100) under practical conditions must be covered with many water molecules at low temperature; besides, O_2 molecule filling V_{Oas} and hydroxyl group can also be present at α-MoO_3 (100) under practical gas sensing measurement if considering interaction between O_2, H_2O and V_O.

Acknowledgements

This research is supported by the Hubei Provincial Natural Science Foundation of China (No. 2020CFB188), Sanya Science and Education Innovation Park of Wuhan University of Technology (No. 2020KF0030), National Natural Science Foundation of China (No. 62171331), the Key Project of Department of Education of Guangdong Province (No. 2018KCXTD026) and the Deanship of Scientific Research (DSR) at King Abdulaziz University of Jeddah (No. KEP-MSc-70-130-42). Thanks to the computational support by Research Centre for Materials Genome Engineering in Wuhan University of Technology.

References

1. Yang, S.; Liu, Y.; Chen, W.; Jin, W.; Zhou, J.; Zhang, H.; Zakharova, G. S., High Sensitivity and Good Selectivity of Ultralong MoO_3 Nanobelts for Trimethylamine Gas. *Sensors and Actuators B: Chemical* **2016**, *226*, 478-485.

2. Kwak, D.; Wang, M.; Koski, K. J.; Zhang, L.; Sokol, H.; Maric, R.; Lei, Y., Molybdenum Trioxide (α-MoO_3) Nanoribbons for Ultrasensitive Ammonia (NH_3) Gas Detection: Integrated Experimental and Density Functional Theory Simulation Studies. *ACS Applied Materials & Interfaces* **2019**, *11*, 10697-10706.

3. Cho, Y. H.; Ko, Y. N.; Kang, Y. C.; Kim, I.-D.; Lee, J.-H., Ultraselective and Ultrasensitive Detection of Trimethylamine Using MoO_3 Nanoplates Prepared by Ultrasonic Spray Pyrolysis. *Sensors and Actuators B: Chemical* **2014**, *195*, 189-196.

4. Chu, X.; Liang, S.; Sun, W.; Zhang, W.; Chen, T.; Zhang, Q., Trimethylamine Sensing Properties of Sensors Based on MoO_3 Microrods. *Sensors and Actuators B: Chemical* **2010**, *148*, 399-403.

5. Sui, L.; Song, X.; Cheng, X.; Zhang, X.; Xu, Y.; Gao, S.; Wang, P.; Zhao, H.; Huo, L., An Ultraselective and Ultrasensitive Tea Sensor Based on α-MoO_3 Hierarchical Nanostructures and the Sensing Mechanism. *CrystEngComm* **2015**, *17*, 6493-6503.

6. Sui, L.-l.; Xu, Y.-M.; Zhang, X.-F.; Cheng, X.-L.; Gao, S.; Zhao, H.; Cai, Z.; Huo, L.-H., Construction of Three-Dimensional Flower-Like α-MoO_3 with Hierarchical Structure for Highly Selective Triethylamine Sensor. *Sensors and Actuators B: Chemical* **2015**, *208*, 406-414.

7. Srinivasan, P.; Rayappan, J. B. B., Chemi-Resistive Sensing of Methylamine Species Using Twinned α-MoO_3 Nanorods: Role of Grain Features, Activation Energy and Surface Defects. *Sensors and Actuators B: Chemical* **2021**, *349*, 130759.

8. Chithambararaj, A.; Rajeswari Yogamalar, N.; Bose, A. C., Hydrothermally Synthesized h -MoO_3 and α-MoO_3 Nanocrystals: New Findings on Crystal-Structure-Dependent Charge Transport. *Crystal Growth & Design* **2016**, *16*, 1984-1995.

9. Papakondylis, A.; Sautet, P., Ab Initio Study of the Structure of theα-MoO_3 Solid and Study of the Adsorption of H_2O and Co Molecules on Its (100) Surface. *The Journal of Physical Chemistry* **1996**, *100*, 10681-10688.

10. Firment, L. E.; Ferretti, A., Stoichiometric and Oxygen Deficient MoO_3(010) Surfaces. *Surface Science* **1983**, *129*, 155-176.

11. Cavalleri, M.; Hermann, K.; Guimond, S.; Romanyshyn, Y.; Kuhlenbeck, H.; Freund, H. J., X-Ray Spectroscopic Fingerprints of Reactive Oxygen Sites at the MoO_3(010) Surface. *Catalysis Today* **2007**, *124*, 21-27.

12. Tokarz-Sobieraj, R.; Hermann, K.; Witko, M.; Blume, A.; Mestl, G.; Schlögl, R., Properties of Oxygen Sites at the MoO_3(010) Surface: Density Functional Theory Cluster Studies and Photoemission Experiments. *Surface Science* **2001**, *489*, 107-125.

13. Agarwal, V.; Metiu, H., Oxygen Vacancy Formation on α-MoO_3 Slabs and Ribbons. *The Journal of Physical Chemistry C* **2016**, *120*, 19252-19264.

14. Mei, D.; Karim, A. M.; Wang, Y., Density Functional Theory Study of Acetaldehyde Hydrodeoxygenation on MoO_3. *The Journal of Physical Chemistry C* **2011**, *115*, 8155-8164.

15. Coquet, R.; Willock, D. J., The (010) Surface of Alpha- MoO_3, a DFT + U Study. *Physical Chemistry Chemical Physics: PCCP* **2005**, *7*, 3819-28.

16. Chen, M.; Friend, C. M.; Kaxiras, E., The Chemical Nature of Surface Point Defects on MoO_3(010): Adsorption of Hydrogen and Methyl. *Journal of the American Chemical Society* **2001**, *123*, 2224-2230.

17. Brückman, K.; Grabowski, R.; Haber, J.; Mazurkiewicz, A.; Słoczyński, J.; Wiltowski, T., The Role of Different MoO_3 Crystal Faces in Elementary Steps of Propene Oxidation. *Journal of Catalysis* **1987**, *104*, 71-79.

18. Smith, M. R.; Ozkan, U. S., The Partial Oxidation of Methane to Formaldehyde: Role of Different Crystal Planes of MoO_3. *Journal of Catalysis* **1993**, *141*, 124-139.

19. Delley, B., An All‐Electron Numerical Method for Solving the Local Density Functional for Polyatomic Molecules. *The Journal of Chemical Physics* **1990**, *92*, 508-517.

20. Delley, B., From Molecules to Solids with the Dmol3 Approach. *The Journal of Chemical Physics* **2000**, *113*, 7756-7764.

21. Kihlborg, L., Least Squares Refinement of Crystal Structure of Molybdenum Trioxide. *Arkiv for Kemi* **1963**, *21*, 357-+.

22. Pandeeswari, R.; Jeyaprakash, B. G., Nanostructured α-MoO_3 Thin Film as a Highly Selective Tma Sensor. *Biosensors and Bioelectronics* **2014**, *53*, 182-186.

23. https://www.processsensing.com/en-us/humidity-calculator/.

24. Yang, T.; Liu, Y.; Jin, W.; Han, Y.; Yang, S.; Chen, W., Investigation on the Transformation of Absorbed Oxygen at ZnO {10−10} Surface Based on a Novel Thermal Pulse Method and Density Functional Theory Simulation. *ACS Sensors* **2017**, *2*, 1051-1059.

25. Yang, T.; Jin, W.; Liu, Y.; Li, H.; Yang, S.; Chen, W., Surface Reactions of CH_3OH, NH_3 and CO on ZnO Nanorod Arrays Film: DFT Investigation for Gas Sensing Selectivity Mechanism. *Applied Surface Science* **2018**, *457*, 975-980.

26. Kim, K.; Choi, P. g.; Itoh, T.; Masuda, Y., Catalyst-Free Highly Sensitive SnO_2 Nanosheet Gas Sensors for Parts Per Billion-Level Detection of Acetone. *ACS Applied Materials & Interfaces* **2020**, *12*, 51637-51644.

27. Hübner, M.; Pavelko, R. G.; Barsan, N.; Weimar, U., Influence of Oxygen Backgrounds on Hydrogen Sensing with SnO_2 Nanomaterials. *Sensors and Actuators B: Chemical* **2011**, *154*, 264-269.

28. Boepple, M.; Zhu, Z.; Hu, X.; Weimar, U.; Barsan, N., Impact of Heterostructures on Hydrogen Sulfide Sensing: Example of Core-Shell Cuo/$CuFe_2O_4$ Nanostructures. *Sensors and Actuators B: Chemical* **2020**, *321*, 128523.

29. Wang, T.-S.; Wang, Q.-S.; Zhu, C.-L.; Ouyang, Q.-Y.; Qi, L.-H.; Li, C.-Y.; Xiao, G.; Gao, P.; Chen, Y.-J., Synthesis and Enhanced H_2S Gas Sensing Properties of α-MoO_3/CuO P–N Junction Nanocomposite. *Sensors and Actuators B: Chemical* **2012**, *171-172*, 256-262.

30. Hübner, M.; Simion, C. E.; Tomescu-Stănoiu, A.; Pokhrel, S.; Bârsan, N.; Weimar, U., Influence of Humidity on CO Sensing with p-Type CuO Thick Film Gas Sensors. *Sensors and Actuators B: Chemical* **2011**, *153*, 347-353.

31. Degler, D.; Junker, B.; Allmendinger, F.; Weimar, U.; Barsan, N., Investigations on the Temperature-Dependent Interaction of Water Vapor with Tin Dioxide and Its Implications on Gas Sensing. *ACS Sensors* **2020**, *5*, 3207-3216.

32. Wicker, S.; Guiltat, M.; Weimar, U.; Hémeryck, A.; Barsan, N., Ambient Humidity Influence on CO Detection with SnO_2 Gas Sensing Materials. A Combined DRIFTS/DFT Investigation. *The Journal of Physical Chemistry C* **2017**, *121*, 25064-25073.

Supporting Information

Surface chemistry of α-MoO_3 (100) and its active site for amines adsorption through density functional calculation

Tingqiang Yang,[a,b,d,] Shuang Yang,[b] Wei Jin,[c] Yule Zhang,[d] Nicolae Barsan,[e] Anne Hemeryck,[f] Wageh Swelm,[g] Ahmed A. Al-Ghamdi,[g] Yueli Liu,[c] Jing Zhou,[b] Wen Chen,[b,]* and Han Zhang[d,]**

[a]Postdoctoral Innovation Practice Base of Guangdong Province, Hanshan Normal University, Chaozhou, 521041, China

[b]State Key Laboratory of Advanced Technology for Materials Synthesis and Processing, School of Materials Science and Engineering, Wuhan University of Technology, Wuhan, 430070, China

[c]State Key Laboratory of Silicate Materials for Architectures, School of Materials Science and Engineering, Wuhan University of Technology, Wuhan, 430070, China

[d]Institute of Microscale Optoelectronics, Collaborative Innovation Centre for Optoelectronic Science & Technology, Key Laboratory of Optoelectronic Devices and Systems of Ministry of Education and Guangdong Province, College of Physics and Optoelectronic Engineering, Shenzhen Key Laboratory of Micro-Nano Photonic Information Technology, Guangdong Laboratory of Artificial Intelligence and Digital Economy (SZ), Shenzhen University, Shenzhen, 518060, China

[e]Institute of Physical and Theoretical Chemistry and Center for Light-Matter Interaction, Sensors & Analytics (LISA+), University of Tübingen, D-72076 Tübingen, Germany

[f]LAAS-CNRS, Université de Toulouse, CNRS, F-31555 Toulouse, France

[g]Department of Physics, Faculty of Science, King Abdulaziz University, Jeddah 21589, Saudi Arabia

*Corresponding author:

Dr. Tingqiang Yang: yang_tq@szu.edu.cn

Prof. Wen Chen: chenw@whut.edu.cn

Prof. Han Zhang: hzhang@szu.edu.cn

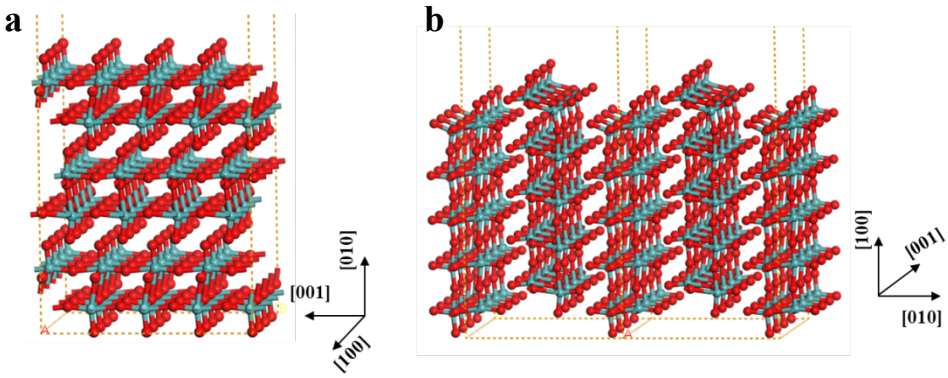

Figure S1 (a) (4 × 4) supercell of α-MoO_3 (010) surface, (b) (1 × 4) supercell of α-MoO_3 (100) surface showing two periodic lattice in [010] direction.

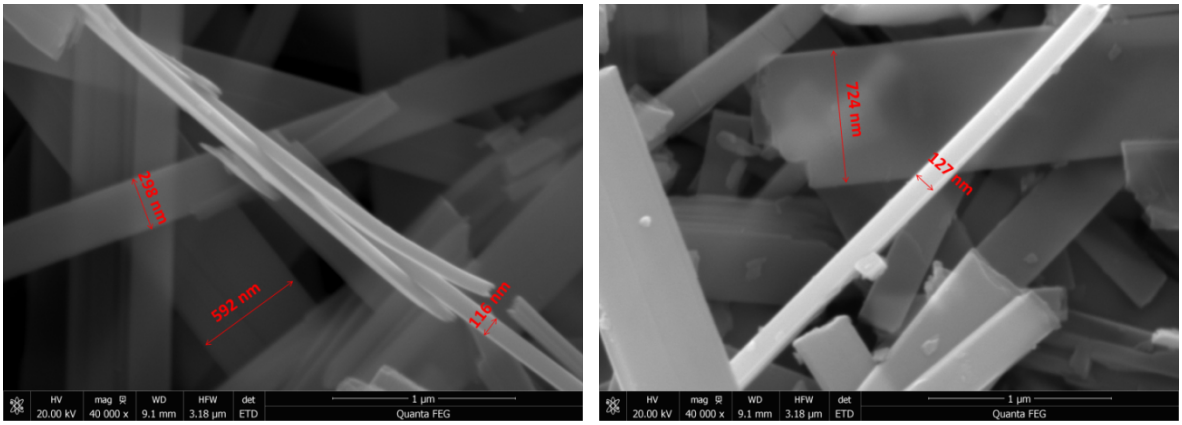

Figure S2 Field emission scanning electron microscope (FESEM) images of our α-MoO_3 nanobelts

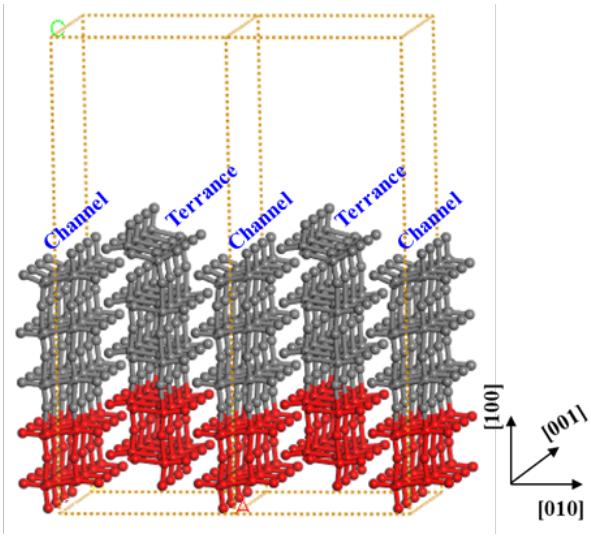

Figure S3 α-MoO_3 (100) slab with a 15 Å vacuum layer (The relaxed atoms is in grey and the fixed in red.)

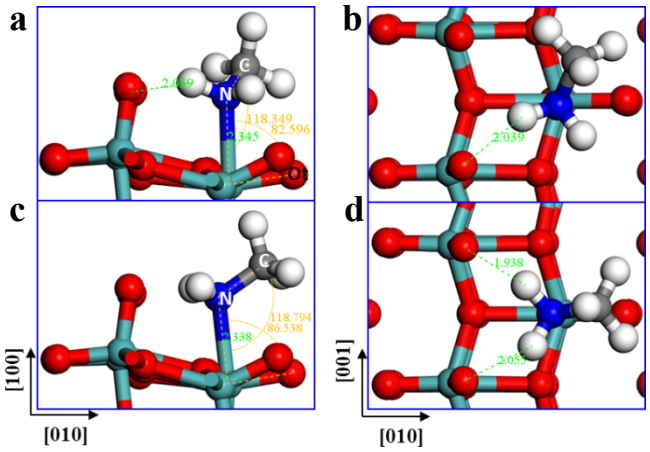

Figure S4 Two configurations for MMA adsorption at terrace of α-MoO_3 (100): (a, b) N−C bond not overlapping with Mo−O_t bond and (c, d) N−C bond overlapping with Mo−O_t bond in the view from [100] direction.

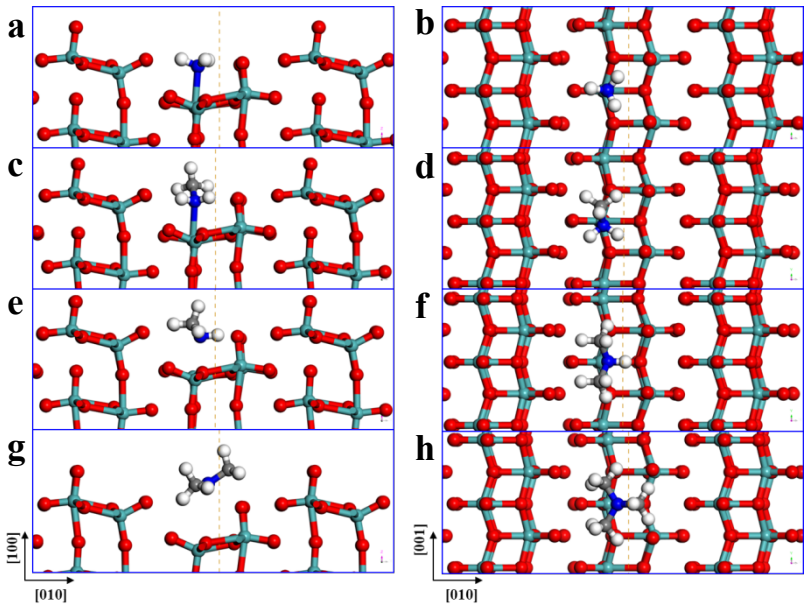

Figure S5 Adsorption configuration at channel of α-MoO_3 (100): (a, b) NH_3, (c, d) MMA, (e, f) DMA, and (g, h) TMA.

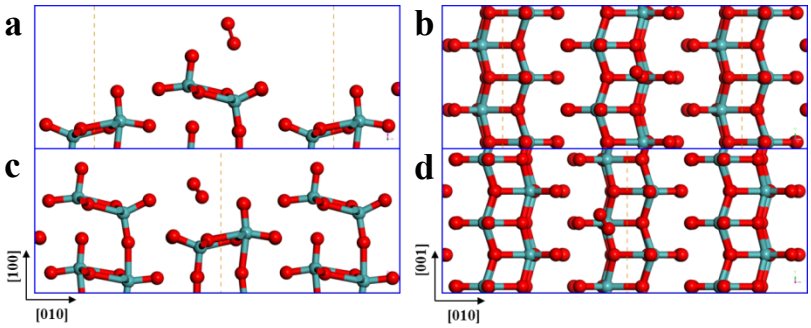

Figure S6 O_2 adsorption configuration at α-MoO_3 (100): (a, b) Terrace and (c, d) channel.

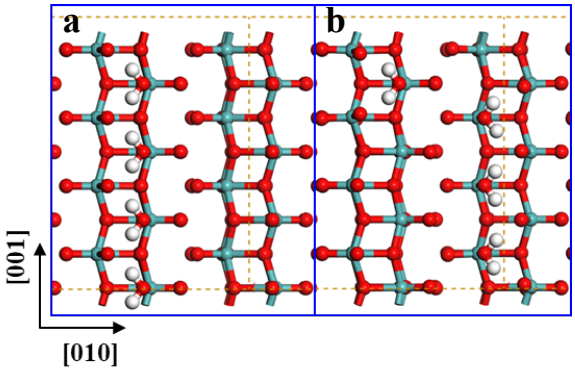

Figure S7 Two other configurations of 1/2 coverage of water: (a) All of four water molecules are adsorbed at terrace, (b) one at terrace and three at channel.

The E_{ads} for **Figure S7a** and **S7b** is respectively −1.05 eV and −1.15 eV, compared with −1.16 eV of **Figure 3e**.

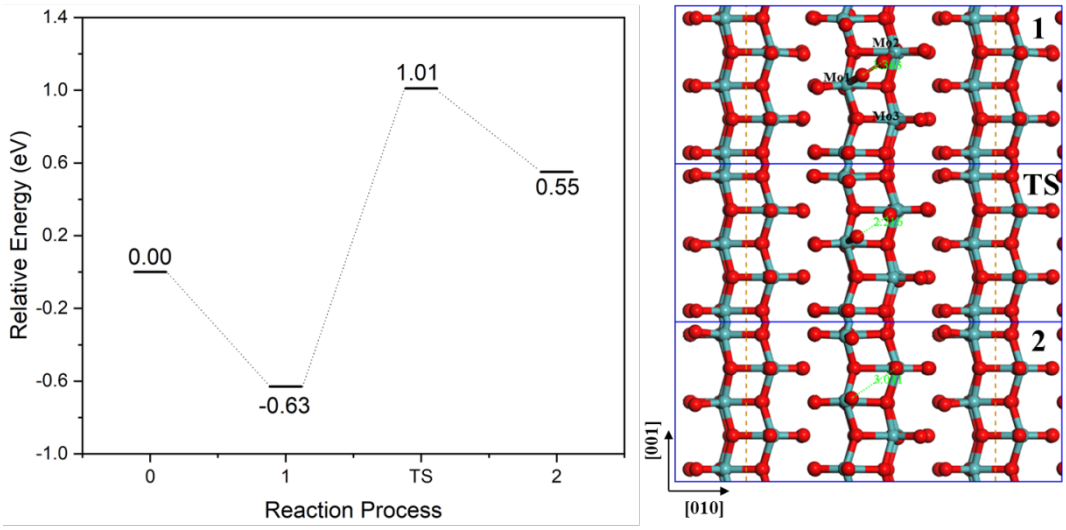

Figure S8 Adsorption and dissociation process of O_2 at α-MoO_3 (100) with one $V_{Oas(t)}$. The left shows relative energy at each process with reference to overall energy of defective surface and vapor O_2 molecule, and the right shows atomic structure in different process.

Because of surface symmetry, adsorption configuration by interacting with Mo1 and Mo2 is same as that with Mo1 and Mo3.

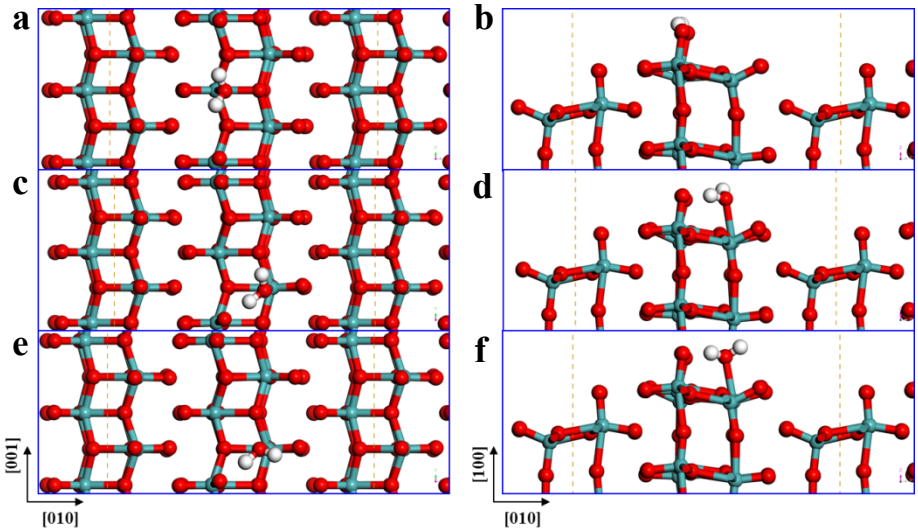

Figure S9 Water adsorption at α-MoO_3 (100) with one $V_{Oas(t)}$: (a, b) at vacancy and (c-f) beside vacancy but a little different in configuration.

The E_{ads} for (a, b), (c, d) and (e, f) is respectively −0.96 eV, −1.00 eV, and −1.06 eV.